CrystEngComm

Cite this: *CrystEngComm*, 2011, **13**, 6036

www.rsc.org/crystengcomm

COMMUNICATION

Electrochemical growth of vertically aligned ZnO nanorod arrays on oxidized bi-layer graphene electrode†

Chunju Xu,[a] Jae-Hyun Lee,[a] Jong-Cheol Lee,[a] Byung-Sung Kim,[a] Sung Woo Hwang*[b] and Dongmok Whang*[ab]

Received 8th June 2011, Accepted 3rd August 2011
DOI: 10.1039/c1ce05695f

Vertically aligned ZnO nanorod arrays were directly grown on flexible and transparent oxidized bi-layer graphene electrodes by seedless electrochemical deposition. Oxidized defects on the graphene surface induce epitaxial growth of highly dense single crystal ZnO nanorods. The diameter, length as well as morphology of the nanorods can be effectively controlled by adjusting reaction conditions.

Graphene-based one-dimensional (1D) ZnO nanostructures have attracted considerable attention since both of graphene and ZnO have great potential for applications in various transparent and/or flexible optoelectronic devices.[1,2] In the hybrid ZnO–graphene devices, graphene can be used as the transparent and flexible electrode and 1D ZnO nanostructures can behave as active components for the optoelectronic devices. Furthermore, the hybrid structure may enhance the properties of individual material, resulting in significant improvement of its device characteristics.[3,4]

Previously, several methods including metal–organic vapour-phase epitaxy, solution approach and electrochemical route have been reported for growing a 1D ZnO nanostructure on graphene.[2–7] Among them, the electrochemical approach is particularly promising due to its relative low temperature, low-cost, and rapid growth.[8,9] In previous reports, ZnO NRs were electrochemically grown on graphene using an additional ZnO seed layer, oxygen (O_2) bubble or supporting electrolyte.[2,4] However, the disordered polycrystalline ZnO seeds may hinder facile carrier transport between NR and graphene, which is critical for utilizing such a hybrid structure in optoelectronic devices.[7,10] In addition, introduction of an O_2 bubble makes the synthetic process complicated, and anions from the supporting electrolyte would also influence the growth of ZnO NRs.[11] Thus, a low-cost controllable growth of well-aligned ZnO 1D nanostructures on graphene is still crucially needed.

Herein, we report a simple electrochemical approach for growing high-quality vertical ZnO NR arrays directly on oxidized bi-layer graphene electrodes from pure zinc nitrate aqueous solution. The related chemical reactions can be expressed as following: $NO_3^- + H_2O + 2e^- \rightarrow NO_2^- + 2OH^-$ and $Zn^{2+} + 2OH^- \rightarrow ZnO + H_2O$.[12,13] To the best of our knowledge, this is the first report of an electrochemical synthesis of vertical ZnO NR arrays on graphene without a ZnO seed layer, O_2 bubble or electrolyte assistance. The morphology and the aspect ratio of NRs can be easily tuned. In particular, the top surface of the ZnO NR can be controlled from planar hexagonal prisms to tip. Furthermore, the ZnO–graphene hybrid structure exhibits high transparency and flexible properties.

Bi-layer graphene was used as a flexible and transparent electrode because the exposed surface can be chemically modified without losing high conductivity. Single-layer graphene was first grown on Cu foils by chemical vapour deposition (CVD) *via* methane decomposition.[14] The graphene was transferred twice on glass or polyethylene terephthalate (PET) substrates to obtain bi-layer graphene. In order to introduce oxygen defects on the graphene electrode, the upper layer of the bi-layer graphene was then partially oxidized by O_2 plasma treatment. Micro-Raman spectroscopy and X-ray photoelectron spectroscopy (XPS) confirmed that both low-defect unoxidized and oxygen-treated bi-layer graphene were successfully obtained (Fig. S2 and S3†).[15,16] The electrochemical growth of ZnO NRs was carried out in a traditional three-electrode cell. The electrolyte solution contained 0.5∼50 mmol L^{-1} zinc nitrate aqueous solution and current density was controlled from −0.05 to −1.0 mA cm^{-2} for 15∼60 min. Meanwhile, ZnO NRs were also grown on unoxidized graphene or bare ITO under the same conditions for comparison with the oxidized graphene substrate.

Fig. 1 shows that the density and orientation of the ZnO NRs change dramatically on the different chemical status of graphene surface and ITO substrate. ZnO NRs electrochemically grown on unoxidized graphene are of low density and randomly oriented (Fig. 1a). Similar to ZnO on unoxidized graphene, orientations of ZnO NRs grown on amorphous ITO electrode are also random (Fig. 1b). When oxidized graphene electrode is used, however, high density ZnO NR arrays are grown with perfect vertical alignment (Fig. 1c). The average length of ZnO NRs is about 1.1 μm, the diameter of single ZnO NR ranges from 200 to 250 nm and the diameters exhibit uniformally from bottom to top for an arbitrary

[a]*School of Advanced Materials Science & Engineering and Sungkyunkwan Advanced Institute of Nanotechnology, Sungkyunkwan University, Suwon, 440-746, Korea. E-mail: dwhang@skku.edu; Fax: +82-312907410; Tel: +82-312997399*
[b]*Research Center for Time-Domain Nano-functional Devices and School of Electrical Engineering, Korea University, Seoul, 136-701, Korea. E-mail: swhwang@korea.ac.kr; Fax: +82-29210544; Tel: +82-232903241*

† Electronic supplementary information (ESI) available: Experimental details on the synthesis and characterization. Raman and XPS spectra of the bi-layer graphenes before and after O_2 plasma oxidation. SEM images of ZnO seeds in the initial electrodeposition. See DOI: 10.1039/c1ce05695f

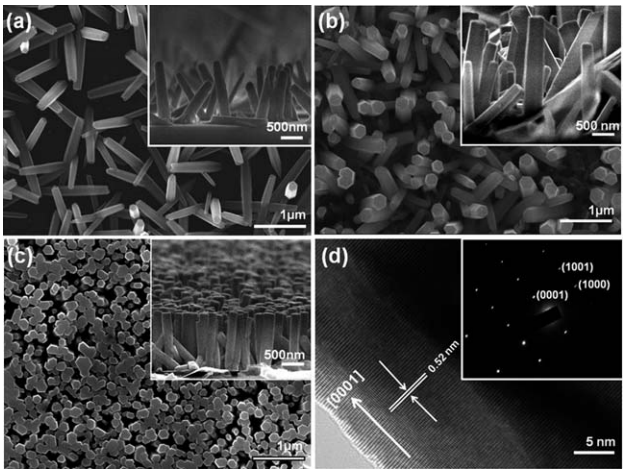

Fig. 1 FESEM images of ZnO NRs electrodeposited from 5 mM Zn $(NO_3)_2$, with an applied current density of −0.15 mA and reaction time of 30 min on (a) unoxidized bi-layer graphene, (b) ITO, and (c) oxidized bi-layer graphene electrode. The insets are the corresponding cross-section views. (d) HRTEM image of a ZnO NR separated from oxidized bi-layer graphene and corresponding SAED pattern in the inset.

ZnO NR. A high-resolution transmission microscopy (HRTEM) image and corresponding selected area electron diffraction (SAED) pattern of single ZnO NR separated from the oxidized graphene electrode demonstrated that the NRs are single crystalline wurtzite ZnO with *c*-axis orientation without dislocations or stacking faults (Fig. 1d). The lattice spacing of 0.52 nm also matches that of the (0001) crystal planes of ZnO, which are perpendicular to the growth direction.

The different growth behaviour between ZnO NRs on the unoxidized and oxidized graphene electrodes could be attributed to the difference in the nucleation process. The lack of a heteroepitaxial relationship between ZnO and the amorphous ITO limited orientation control of the ZnO nanostructures.[8,17] However, ZnO nanostructrures can grow heteroepitaxially on a crystalline graphene surface, as previously reported in the seedless CVD growth of ZnO nanostructures.[6] It is accepted that the formation of ZnO NRs using electrodeposition undergoes initial self-nucleation and subsequent rod growth.[18] In the growth on oxidized graphene, zinc ions in the reactants are coordinated to the oxygen atoms of oxidized graphene surface, resulting in heteroepitaxial growth of ZnO seeds on the graphene surface during the initial nucleation process (Fig. S4a†). In the growth on unoxidized graphene, however, ZnO seeds are primarily formed in the reaction solution and then randomly deposited on the electrode surface because the graphene surface is chemically inert (Fig. S4b†). The vertical growth of ZnO on graphene is highly unlikely when ZnO nanostructures are grown from randomly dispersed ZnO seeds.

In order to investigate the effect of $Zn(NO_3)_2$ concentration on NRs grown on the oxidized graphene electrode, controlled experiments were conducted with various $Zn(NO_3)_2$ concentrations while keeping the other parameters constant. As shown in Fig. 2, vertically well-aligned NRs could be grown under a broad range of concentrations, but the diameter of ZnO NRs becomes smaller when the concentration is decreased. For example, the mean diameter is ~450 nm at the higher concentration of 50 mM (Fig. 2a), and the diameter is reduced to ~100 nm at the lower concentration of 0.5 mM (Fig. 2c). The length variation of the ZnO NRs has the same tendency as that of the diameter (see insets Fig. 2a–c). Higher concentrations of precursor may induce agglomeration of seeds, which results in longer NRs with larger diameters. Interestingly, the morphology of the ZnO NRs is also related to the $Zn(NO_3)_2$ concentration. When the concentration is higher than 5 mM, the top surfaces of NRs show perfect hexagonal facets and the diameters are uniform along the growth direction (Fig. 1 and Fig. 2a). When the concentration is diluted to 1 mM, however, the NR diameter becomes thinner, gradually from bottom to top (Fig. 2b). With further dilution of the solution to 0.5 mM, the top end of the NRs become much sharper and form a needle-like structure (Fig. 2c), which may be readily used in field emission emitters.[6] Formation of such a needle-like morphology in dilute solution is probably due to the gradual depletion of Zn^{2+} and NO_3^- ions during the deposition.

The influence of deposition time on the growth of ZnO NR was also investigated. FESEM images of ZnO NRs deposited for 15 and 60 min show that average length increased from 0.9 μm to 1.4 μm (Fig. 3a–b), whereas the diameters remained largely unchanged (~250 nm). This result indicates that, under the same current density, the diameter of NRs was mainly controlled by the initial formation of ZnO seeds decided by the precursor concentration.

The NR morphology can be also controlled by the applied current density. As the negative current density was increased from −0.05 to −0.5 mA cm^{-2}, NRs with increasing sizes formed (Fig. 1a, Fig. 3c–d). With further increase of current density to −1.0 mA cm^{-2}, all the NRs connected to each other and the top surface exhibited a patch-like shape (not shown). The reason for this is that probably the higher

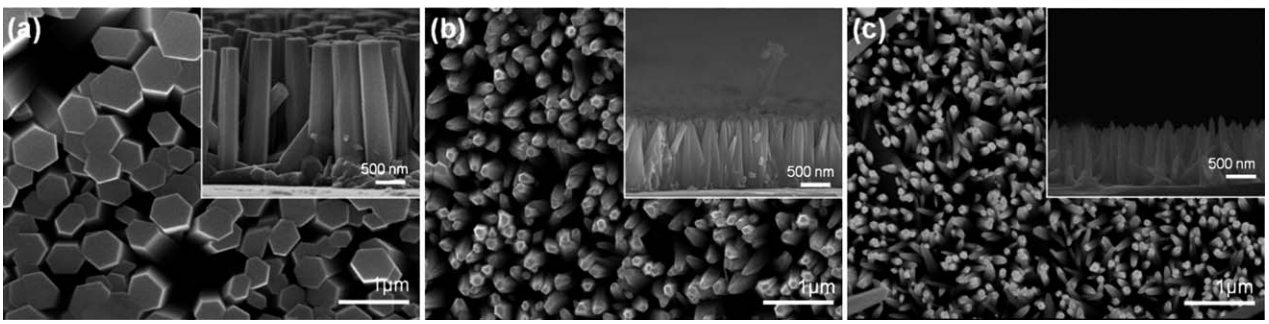

Fig. 2 FESEM images of ZnO NRs electrodeposited under an applied current density of −0.15 mA and reaction time of 30 min on graphene/glass (G/G) obtained with $Zn(NO_3)_2$ concentrations of (a) 50 mM, (b) 1 mM and (c) 0.5 mM. The insets show the cross-section views.

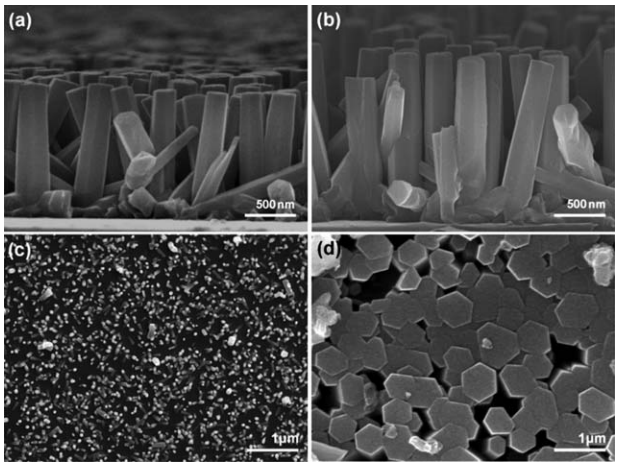

Fig. 3 FESEM images of ZnO NRs deposited from 5 mM precursor on G/G for (a) 15 min and (b) 1 h with current density of 0.15 mA, (c) 0.05 mA and (d) 0.5mA were used with deposition time of 30 min.

current density leads to a rapid formation of OH^- ions at the surface of cathode, which then may result in much denser and larger seeds in the early stage of the growth process.

The optical properties of NRs grown on ITO and graphene were examined by UV-vis and PL spectroscopy at room temperature. Fig. 4a shows that NRs grown on oxidized graphene has only one strong near-band-edge (NBE) emission peak centered at ~380 nm indicating high crystallinity and chemical purity, whereas defect-related strong visible luminescence is observed for NRs grown on bare ITO. It has been reported that the intensity of visible luminescence is associated with defects in ZnO.[19] Previous reports have shown that vertical growth and high surface area improve the UV emission and restrain visible luminescence.[17] As shown in the Fig.1b and c, the ZnO nanorods on oxidized graphene have better vertical alignment and higher density compared to those on the ITO substrate, which results in excellent optical properties for ZnO nanorods on oxidized graphene. Significantly, high-density ZnO NRs on graphene/glass and graphene/PET hold high optical transmittance above 80% at 550 nm (Fig. 4b). The high transparency of ZnO–graphene hybrid can be ascribed to (i) high transparent graphene layer and (ii) the vertical alignment and uniform length of the NRs. Because of the high mechanical flexibility of the graphene/PET substrate, the optical characteristics and structural integrity are well-maintained after repeated severe bending of the hybrid substrate (right inset Fig. 4b). In addition, the electric contact resistance between ZnO NRs and graphene electrode should be reasonably low, since the reproducible and controllable growth of ZnO NRs without a good electrical contact is highly unlikely.

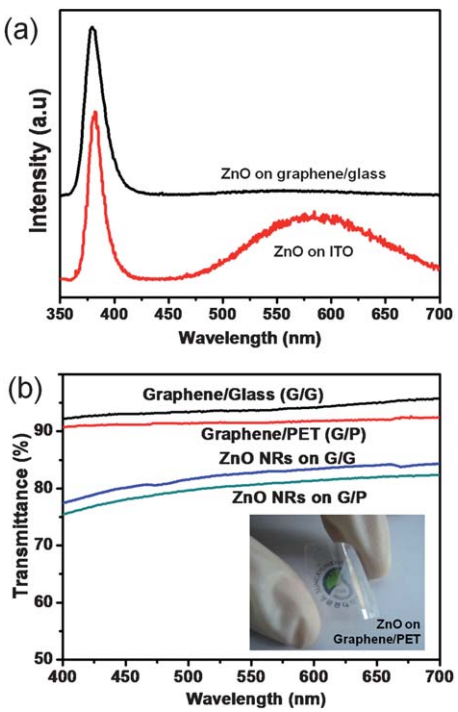

Fig. 4 (a) Room-temperature PL spectra of ZnO NRs on G/G and on ITO. (b) Optical transmittance spectra of G/G, G/PET, ZnO NRs on G/G and on G/PET, inset shows the optical image of ZnO on G/PET, illustrating its transparence and flexibility.

In conclusion, highly dense vertical ZnO NRs were directly grown on an oxidized bi-layer graphene electrode by seedless electrochemical deposition in pure zinc nitrate solution. Oxide defects on the graphene surface induce epitaxial growth of single crystal ZnO NRs on the graphene layer. The diameter, length as well as morphology of the nanorods could be effectively controlled by adjusting reaction conditions, such as current density, precursor concentration, and reaction time. The ZnO–graphene heterojunction nanostructure exhibits outstanding transparency and high flexibility and has the potential to be a platform in transparent and flexible optoelectronic devices.

Acknowledgements

This work was supported by the National Research Foundation of Korea (NRF) grant funded by the Korean Government (MEST) (2009-0076599, 2011-0006268, 2011-0000427).

Notes and references

1 K. Chung, C. H. Lee and G. C. Yi, *Science*, 2010, **330**, 655.
2 Z. Yin, S. Wu, X. Zhou, X. Huang, Q. Zhang, F. Boey and H. Zhang, *Small*, 2010, **6**, 307–312.
3 J. M. Lee, Y. B. Pyun, J. Yi, J. W. Choung and W. I. Park, *J. Phys. Chem. C*, 2009, **113**, 19134–19138.
4 S. Wu, Z. Yin, Q. He, X. Huang, X. Zhou and H. Zhang, *J. Phys. Chem. C*, 2010, **114**, 11816–11821.
5 J. O. Hwang, D. H. Lee, J. Y. Kim, T. H. Han, B. H. Kim, M. Park, K. No and S. O. Kim, *J. Mater. Chem.*, 2011, **21**, 3432–3437.
6 Y.-J. Kim, J.-H. Lee and G.-C. Yi, *Appl. Phys. Lett.*, 2009, **95**, 213101–213103.
7 Y.-J. Kim, Hadiyawarman, A. Yoon, M. Kim, G.-C. Yi and C. Liu, *Nanotechnology*, 2011, **22**, 245603–245610.
8 R. Konenkamp, C. W. Robert and C. Schlegel, *Appl. Phys. Lett.*, 2004, **85**, 6004–6006.
9 G.-R. Li, C.-R. Dawa, Q. Bu, F.-l. Zhen, X.-H. Lu, Z.-H. Ke, H.-E. Hong, C.-Z. Yao, P. Liu and Y.-X. Tong, *Electrochem. Commun.*, 2007, **9**, 863–868.
10 C. J. Novotny, E. T. Yu and P. K. L. Yu, *Nano Lett.*, 2008, **8**, 775–779.
11 L. Xu, Y. Guo, Q. Liao, J. Zhang and D. Xu, *J. Phys. Chem. B*, 2005, **109**, 13519–13522.
12 B. Cao, W. Cai, G. Duan, Y. Li, Q. Zhao and D. Yu, *Nanotechnology*, 2005, **16**, 2567–2574.

13 B. Cao, X. Teng, S. H. Heo, Y. Li, S. O. Cho, G. Li and W. Cai, *J. Phys. Chem. C*, 2007, **111**, 2470–2476.
14 X. Li, W. Cai, J. An, S. Kim, J. Nah, D. Yang, R. Piner, A. Velamakanni, I. Jung, E. Tutuc, S. K. Banerjee, L. Colombo and R. S. Ruoff, *Science*, 2009, **324**, 1312–1314.
15 D. Yang, A. Velamakanni, G. Bozoklu, S. Park, M. Stoller, R. D. Piner, S. Stankovich, I. Jung, D. A. Field and C. A. Ventrice Jr, *Carbon*, 2009, **47**, 145–152.
16 G. Jo, M. Choe, C. Y. Cho, J. H. Kim, W. Park, S. Lee, W. K. Hong, T. W. Kim, S. J. Park and B. H. Hong, *Nanotechnology*, 2010, **21**, 175201.
17 J. Nayak, S. N. Sahu, J. Kasuya and S. Nozaki, *J. Phys. D: Appl. Phys.*, 2008, **41**, 115303.
18 Z. Zhang, G. Meng, Q. Xu, Y. Hu, Q. Wu and Z. Hu, *J. Phys. Chem. C*, 2010, **114**, 189–193.
19 X. Liu, X. Wu, H. Cao and R. P. H. Chang, *J. Appl. Phys.*, 2004, **95**, 3141–3147.